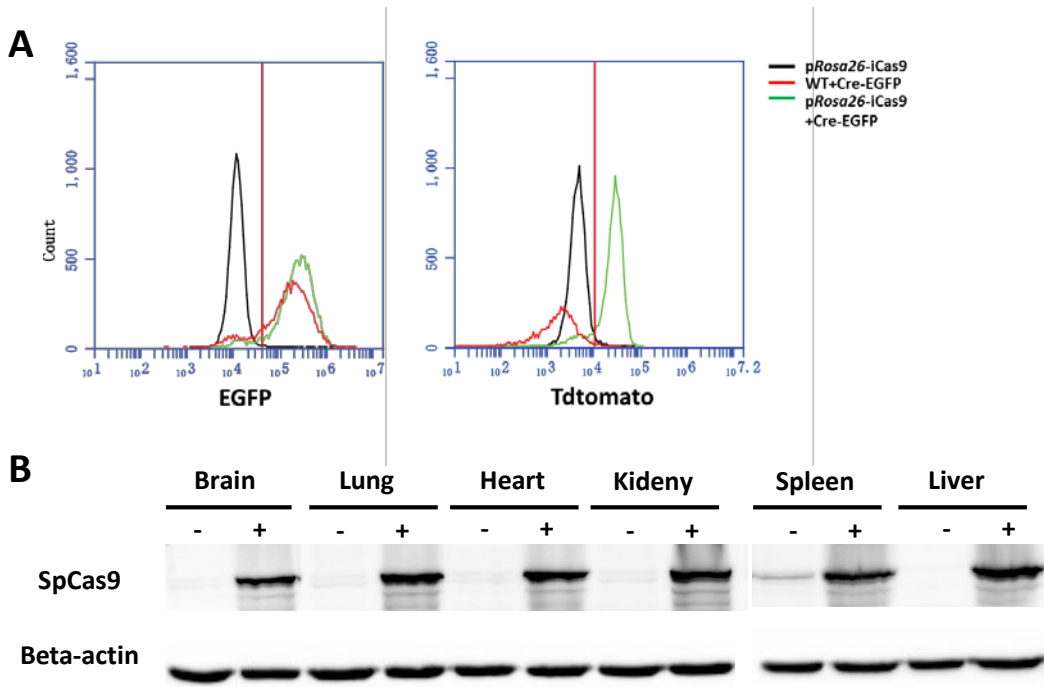
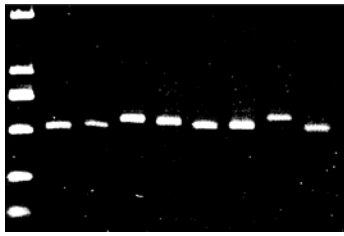
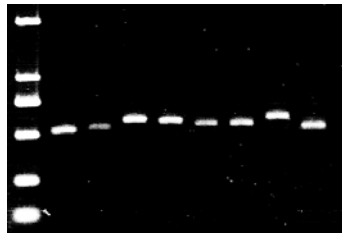
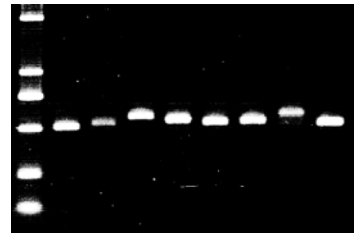
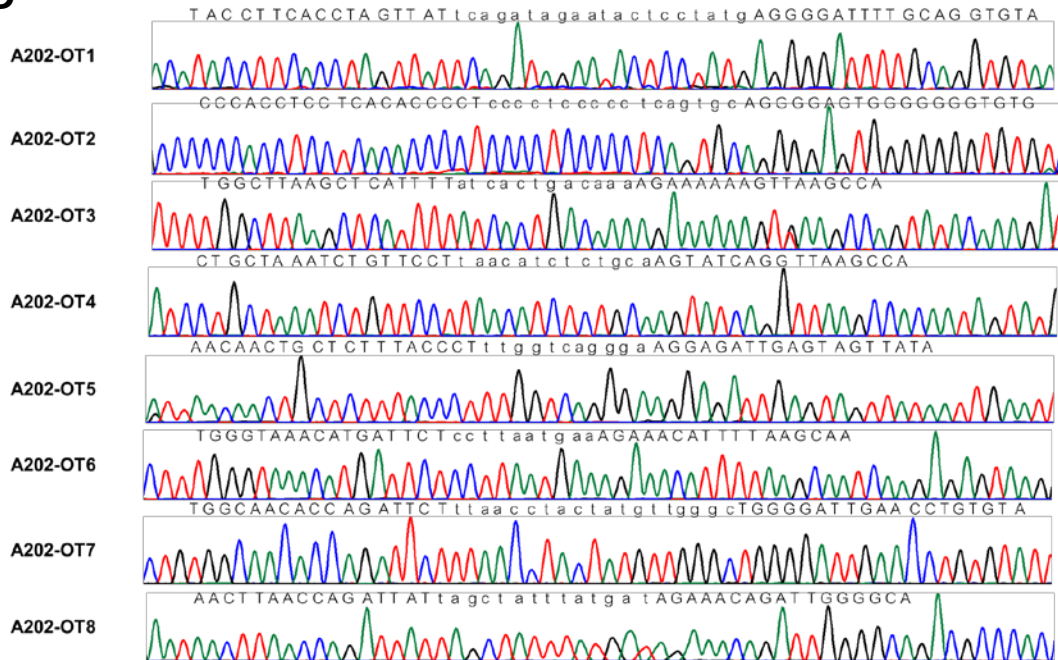
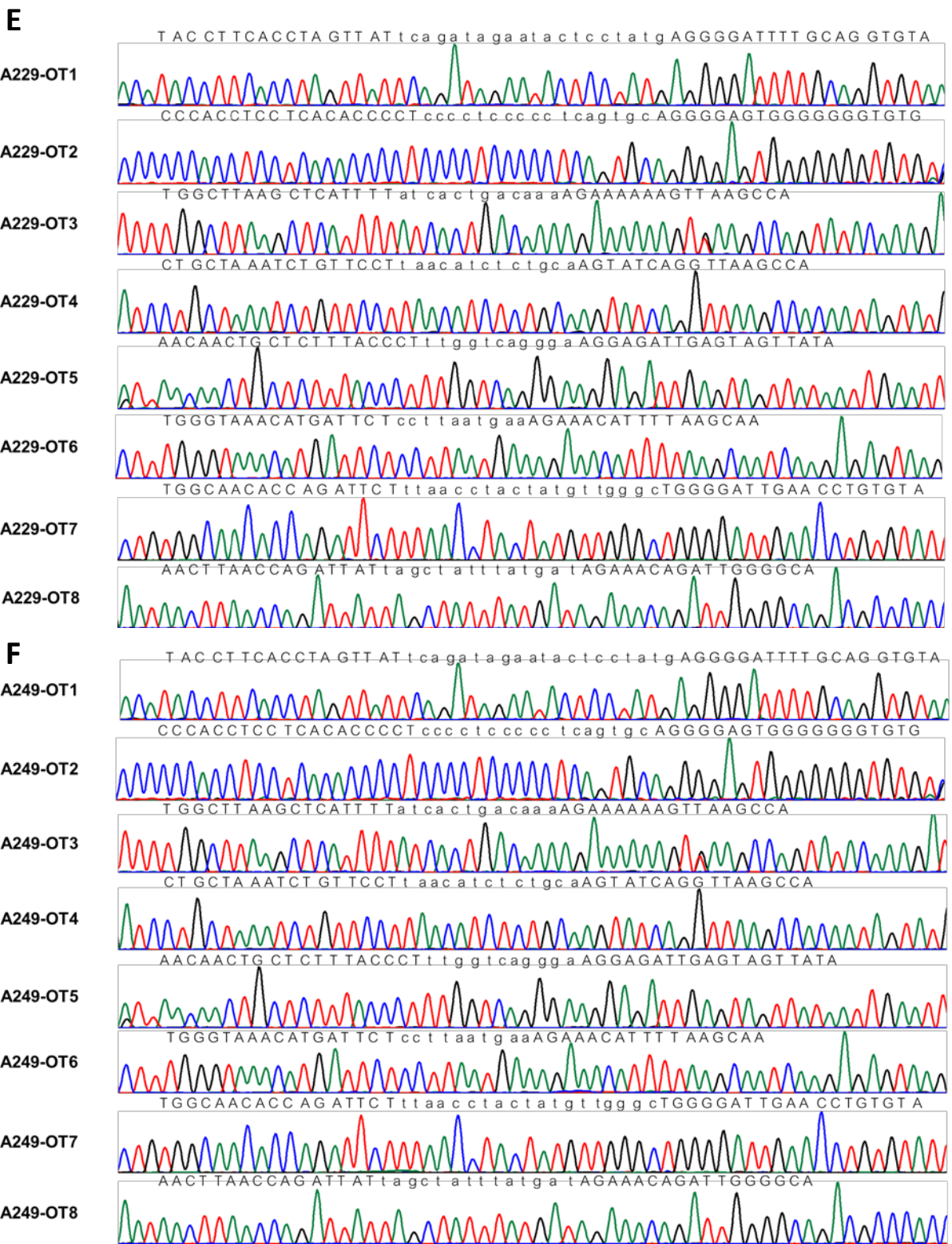


**Supplemental Figure 1.** TALEN-mediated knock-in of Cre-dependent Cas9 expressing cassette into the porcine *Rosa26* locus. (A) Schematic of TALENs targeting the exon 1 and intron 1 of the porcine *albumin* locus. TALEN repeats are colored differently to represent the four repeat variable di-residues (RVD). Each RVD recognizes one cognate-targeted DNA base (NI = A, NG = T, HD = C, NN = G). (B) 5'-junction (1.8 Kb, F1 + R1) and 3'-junction (6.0 Kb, F2 + R2) PCR analyses identified individual colonies with stable knock-in at the porcine *Rosa26* locus. (C) Activation of tdTomato induced by Cre recombinase. Selected cell colonies were infected with Cre-lentivirus and tdTomato were seen 48 h post-transduction. Bright field (left) and tdTomato fluorescence (right); scale bar, 50  $\mu$ m. (D) Summary of *pRosa26*-TALEN-mediated knock-in of Cre-dependent Cas9-expressing cassette into the porcine *Rosa26* locus.

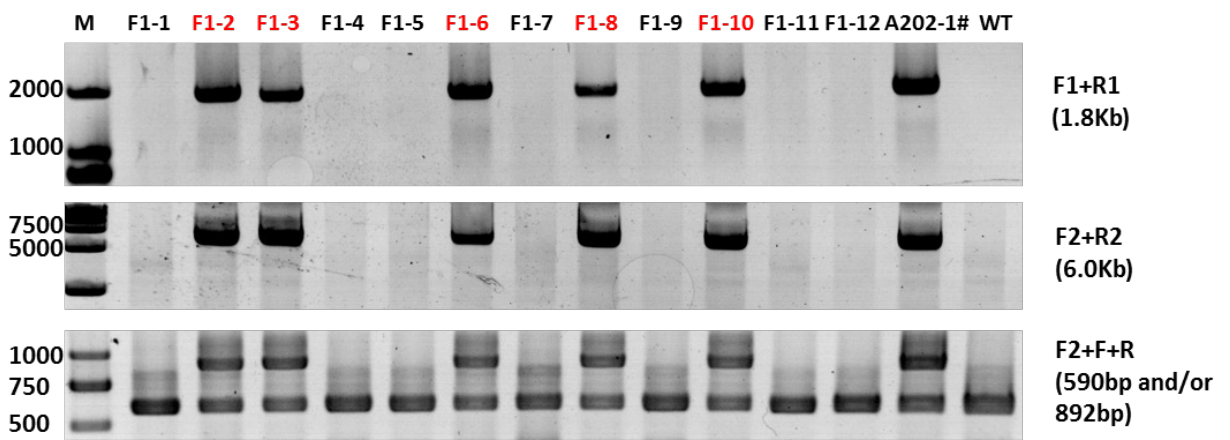
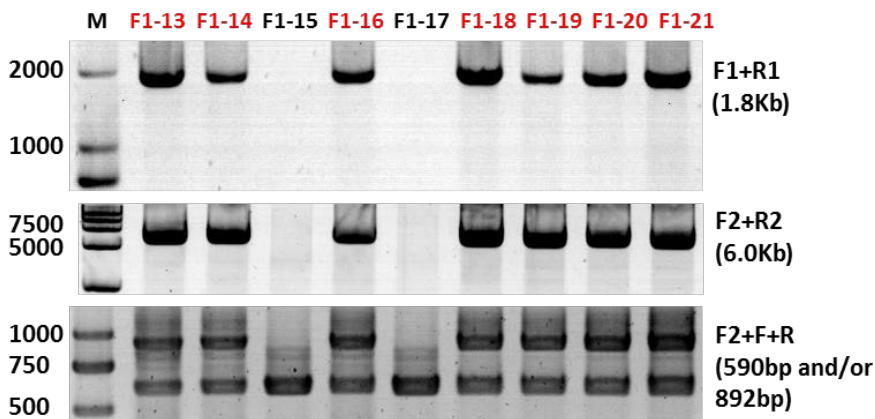


**Supplemental Figure 2.** Activation of SpCas9 in cells isolated from *pRosa26-iCas9* piglets. (A) Flow cytometry histogram of *pRosa26-iCas9* and wild-type fibroblasts infected with Cre-EGFP lentivirus. (B) Western Blot analysis of SpCas9 activation in different primary cells isolated from *pRosa26-iCas9* piglets.

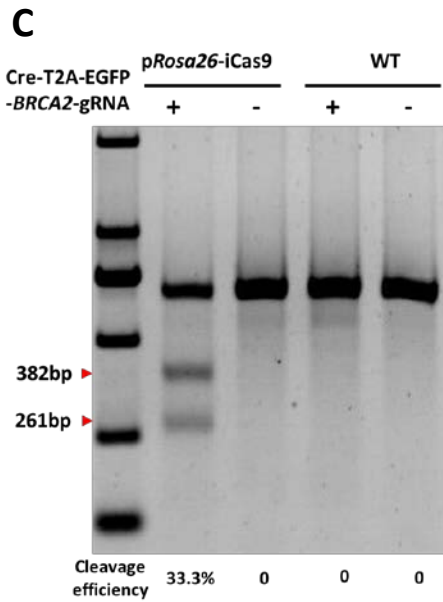
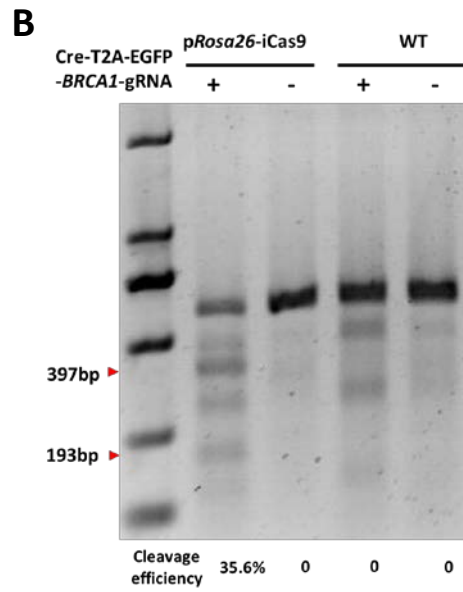
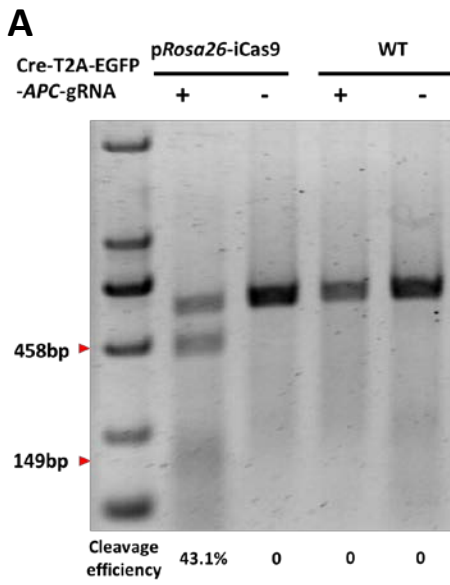
**A** A202-1 OT-1-OT-8**B** A229-1 OT-1-OT-8**C** A249-1 OT-1-OT-8**D**



**Supplemental Figure 3.** Off-target analysis by T7EN1 cleavage assay and Sanger sequencing in all three cloned Cre-dependent Cas9-expressing piglets. T7EN1 assays of the PCR products of eight candidate off-target sites using the genome DNA of three born piglets (A, A202-1#; B, A229-1#; C, A249-1#) as the template. The fragments around the eight potential off-target loci of *pROSA26*-TALEN were then subjected to Sanger sequencing (D, A202-1#; E, A229-1#; F, A249-1#). No off-target locus exists in all three cloned piglets.

**A****B****C**

**Supplemental Figure 4.** Establishment of Cre-dependent Cas9-expressing pig colony by mating the healthy founder pig with two wild-type sows. (A) Twelve F1 Cre-dependent Cas9-expressing piglets, generated through crossbreeding male founders and wild-type sows. (B, C) PCR screening of individuals in F1 generations.



**Supplemental Figure 5.** T7EN1 assays for Cas9-mediated cleavage at *APC* (A), *BRCA1* (B), and *BRCA2* (C) loci in pRosa26-iCas9 and wild-type fibroblasts infected with or without lentivirus AB12.



**A**

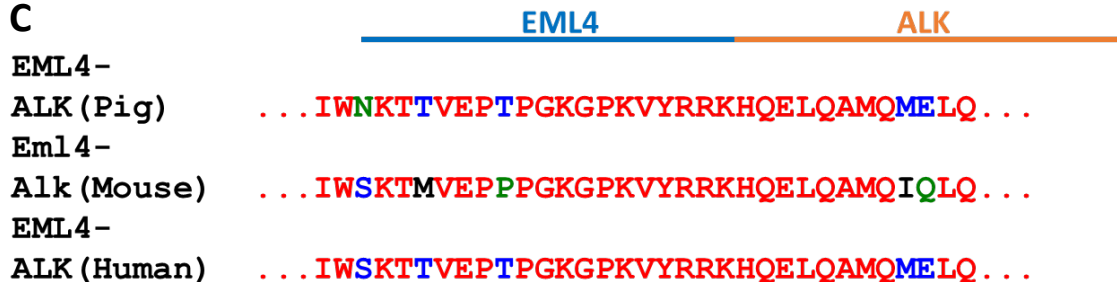
Fig (*ALK*-exon-13) (1) **TGTCGCCACCCCGGAGCCCAAGCTGCCGCTCTCGCTGATTCTCTCCGTGTGACCTCCGCCCTCGTGGCCGCCCTGGTCTGGCCTTCTCCGGCGTCAT**  
 Mouse (*Alk*-exon-19) (1) **TGTCACCCACCCCGGAGCCCACTGCCGCTCTCATTGATCCTCTCCGTGTGACCTCTGCCCTGGTGGCTGCCCTGGTCTGGCATTCTCCGGCATCAT**  
 Human (*ALK*-exon-19) (1) **TGTCACCCACCCCGGAGCCACACTGCCACTCTCGCTGATCCTCTCTGTGTGACCTCTGCCCTCGTGGCCGCCCTGGTCTGGCTTCTCCGGCATCAT**

Fig (*ALK*-exon-13) (101) **GATCG**  
 Mouse (*Alk*-exon-19) (101) **GATTG**  
 Human (*ALK*-exon-19) (101) **GATTG**

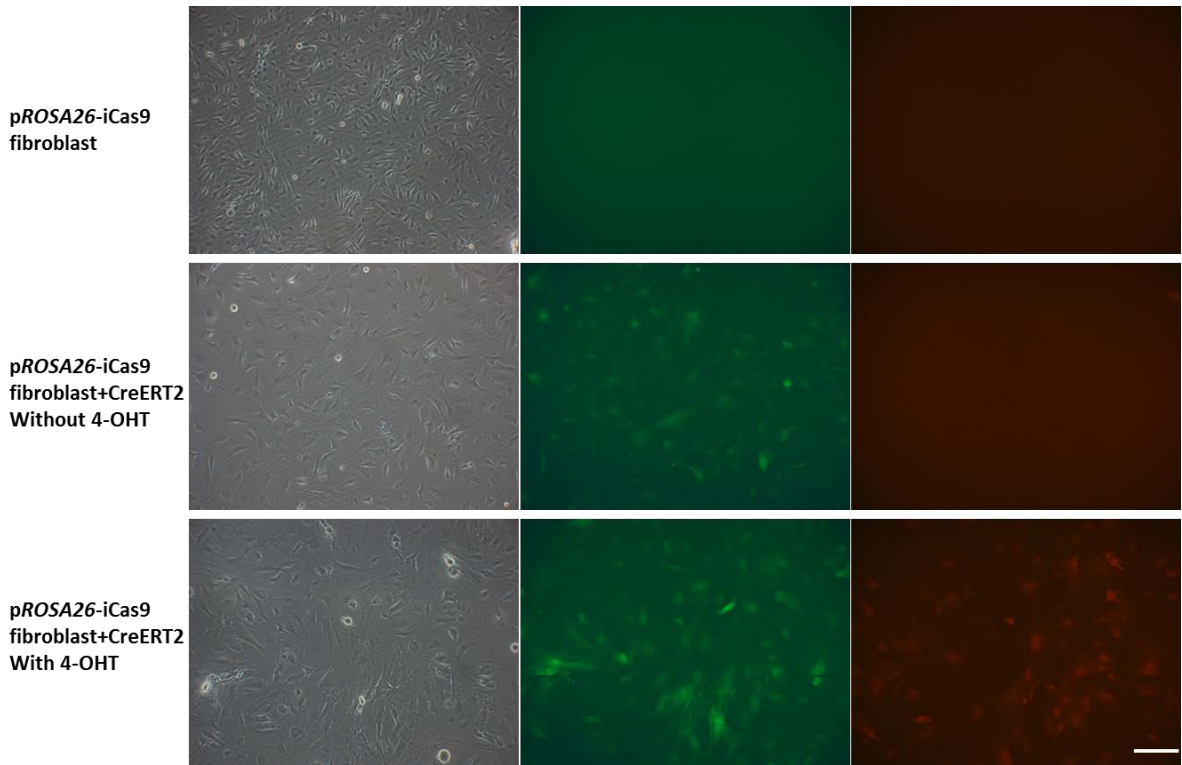
**B**

Fig (*EML4*-exon-14) (1) **AAATATGAAAAACCAAATTTGTGCAGTGTTAGCATTCTGGGGAATGGAGATGTGCTTACTGGAGACTCAGGTGGAATCATACTTATATGGAACAAA**  
 Mouse (*Eml4*-exon-14) (1) **AAATATGAAAAACCAAATTCGTTTCAGTGTTGGCATTCTGGGGAATGGAGATGTTCTCACTGGAGACTCGGGTGGAGTCATGCTGATCTGGAGCAAAA**  
 Human (*EML4*-exon-13) (1) **AAATATGAAAAACCAAATTTGTGCAGTGTTAGCATTCTGGGGAATGGAGATGTTCTTACTGGAGACTCAGGTGGAATCATGCTTATATGGAACAAA**

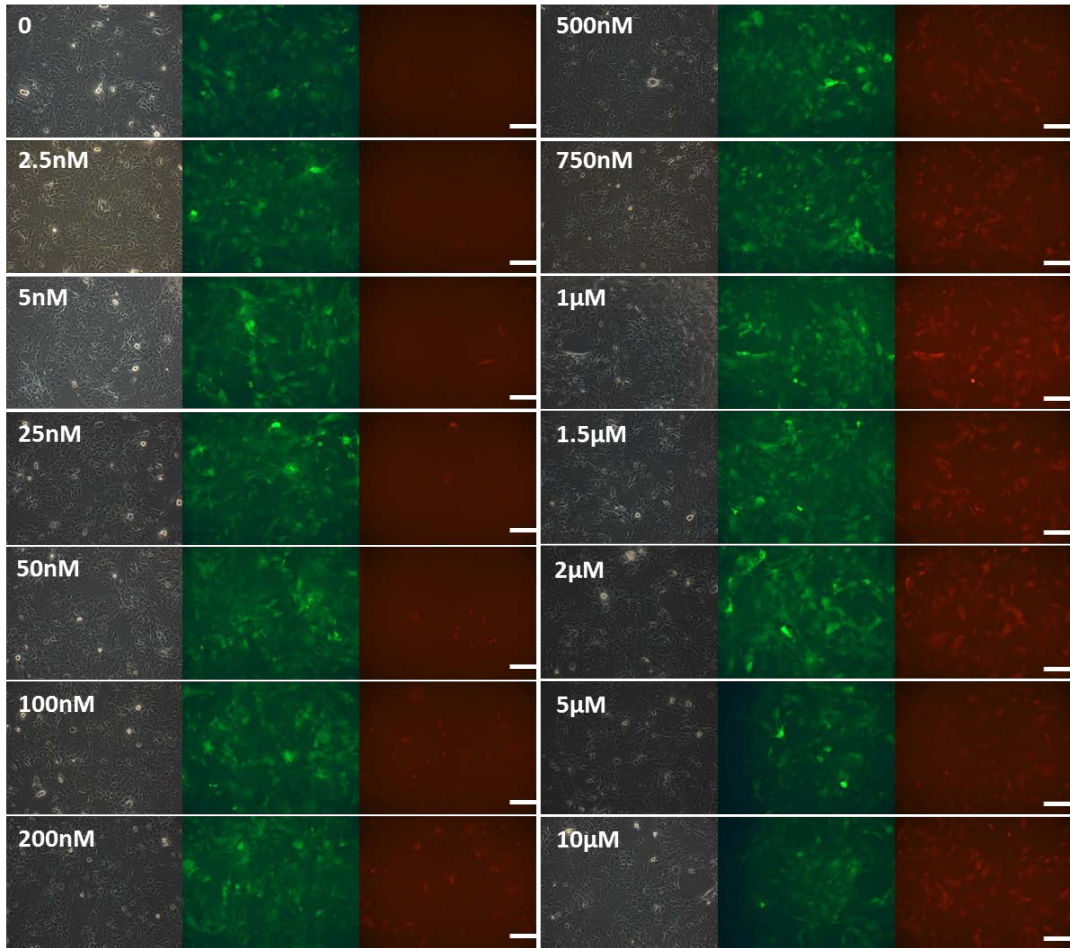
Fig (*EML4*-exon-14) (101) **CTACTGTAGAACCCACACCTGGGAAAGGCAAAAAG**  
 Mouse (*Eml4*-exon-14) (101) **CGATGTTAGAGCCCCCGCCGGGAAAGGACCTAAAG**  
 Human (*EML4*-exon-13) (101) **CTACTGTAGAGCCACACCTGGGAAAGGACCTAAAG**

**C**

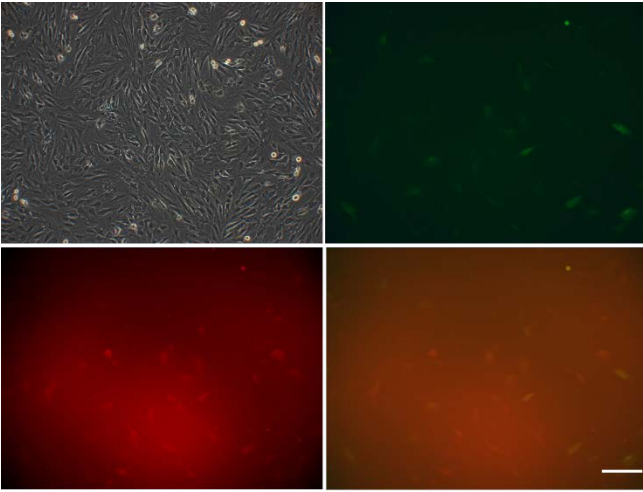
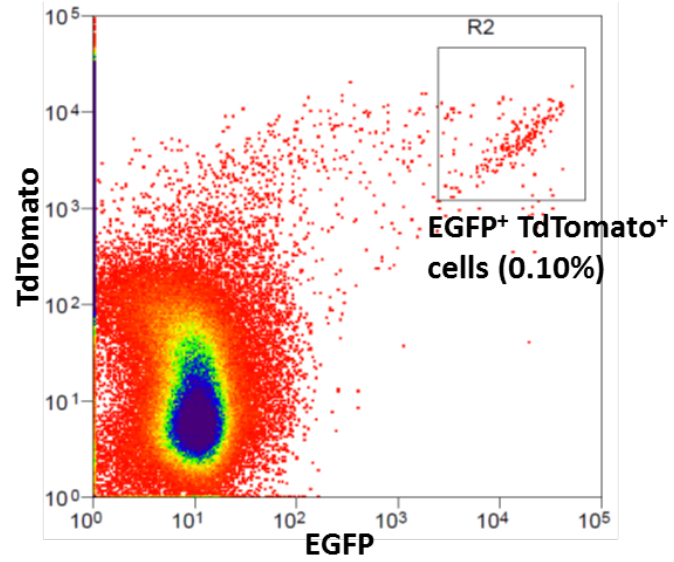
**Supplemental Figure 7.** Human, murine, and porcine *ALK* and *EML4*. (A) Sequence alignment of porcine *ALK* exon 13, human and murine *Alk* exon 19. (B) Sequence alignment of porcine and murine *EML* exon 14, human *EML4* exon 13. (C) Predicted porcine, murine and human *EML4*–*ALK* proteins.



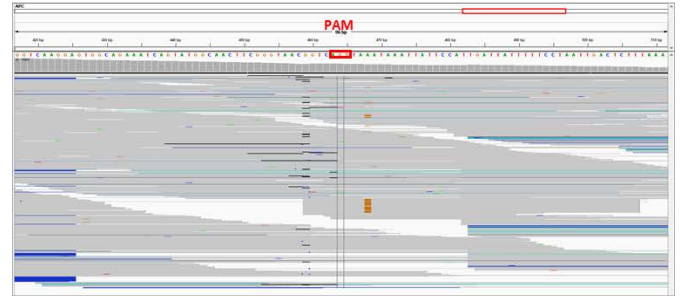
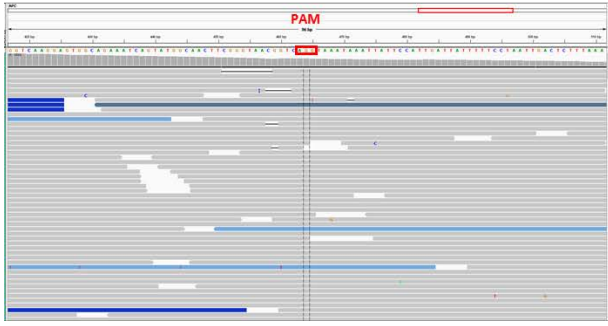
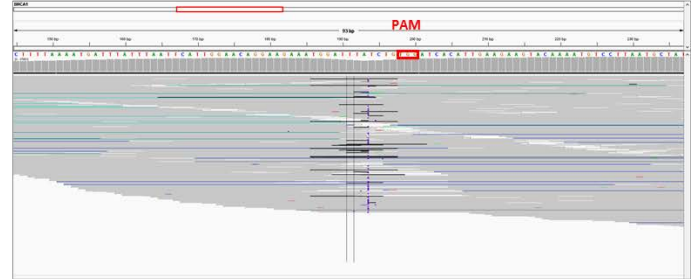
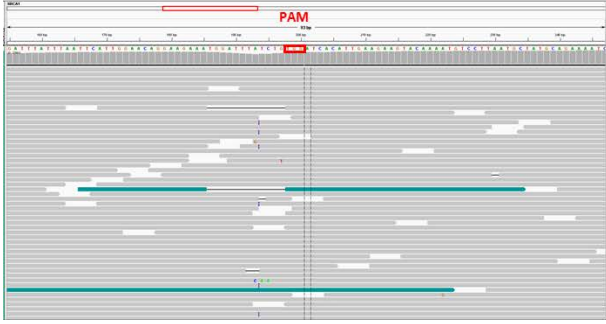
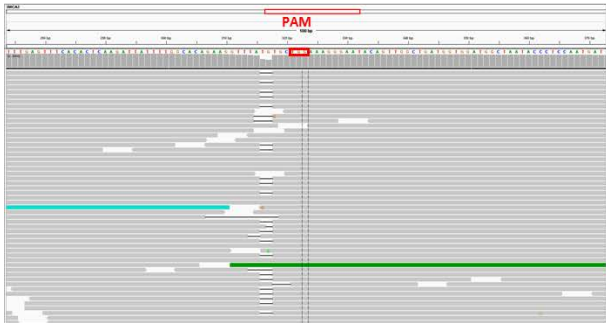
**Supplemental Figure 8.** Bright field (left) and fluorescent images (middle and right) using appropriate filters under fluorescence microscope of p*Rosa26*-iCas9 fibroblasts (upper), p*Rosa26*-iCas9 fibroblasts infected with CreERT2-EGFP lentivirus without 4-OHT treatment (middle), and p*Rosa26*-iCas9 fibroblasts infected with CreERT2-EGFP lentivirus with 4-OHT treatment (bottom).



**Supplemental Figure 9.** Optimization of 4-OHT treatment concentrations. Fluorescences of pRosa26 fibroblasts treated with different 4-OHT concentrations were observed using appropriate filters under the fluorescence microscope. Left, the bright field; middle, EGFP fluorescence; right, tdTomato fluorescence.

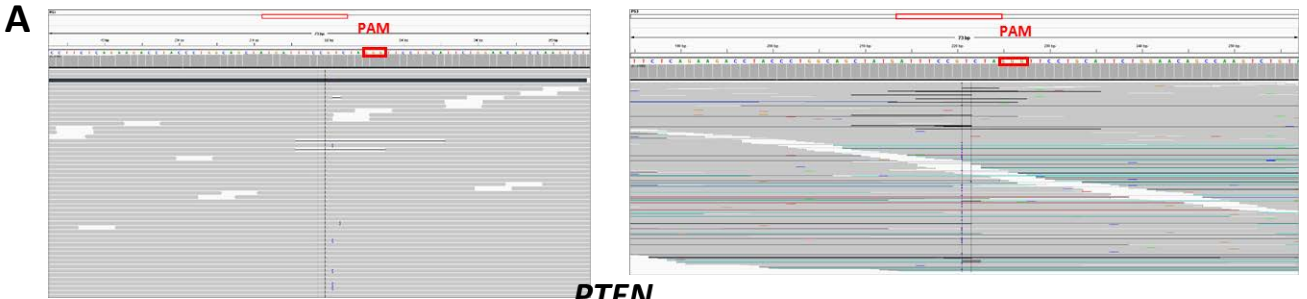
**a****b**

**Supplemental Figure 10.** (A) EGFP and tdTomato-positive cells were observed using a confocal fluorescence microscope. Upper left, bright field; upper right, EGFP fluorescence; bottom left, tdTomato fluorescence; bottom right, merged; scale bars, 50  $\mu\text{m}$ . (B) EGFP and tdTomato-positive cells were successfully sorted out with a frequency of approximately 0.1%.

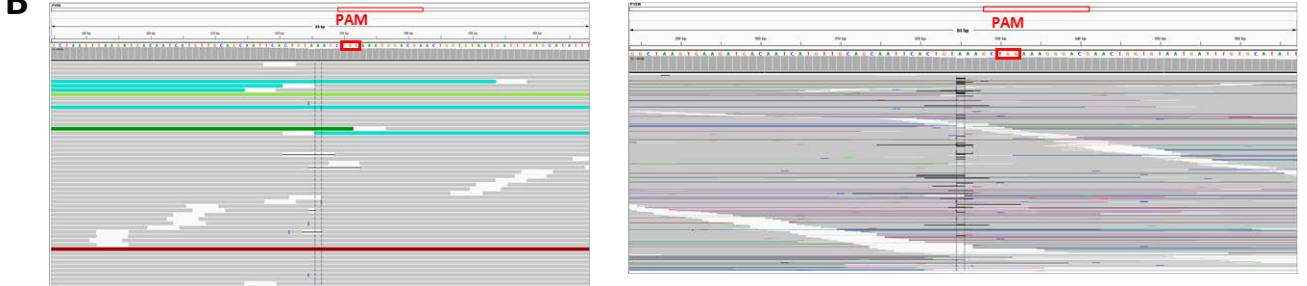
**A****APC****B****BRCA1****C****BRCA2**

**Supplemental Figure 11.** Original deep sequencing results of *APC* (A), *BRCA1* (B), and *BRCA2* (C) of the ear fibroblasts from the ear tissues of Cre-dependent Cas9-expressing pigs infected with lentivirus AB12.

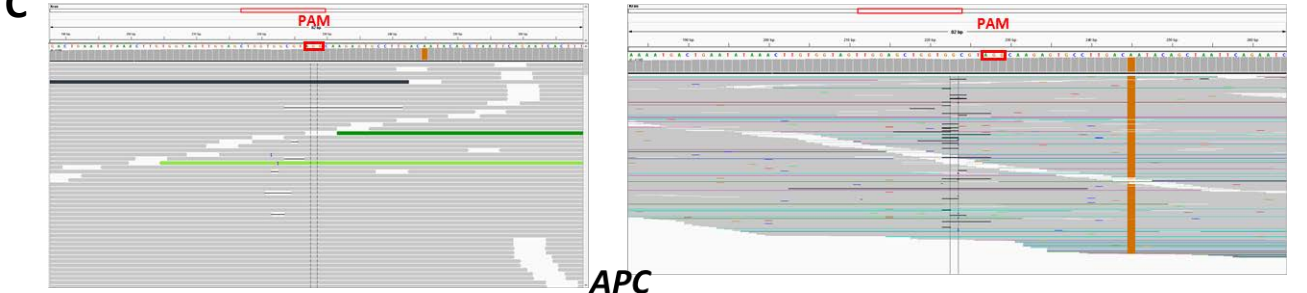
**TP53**



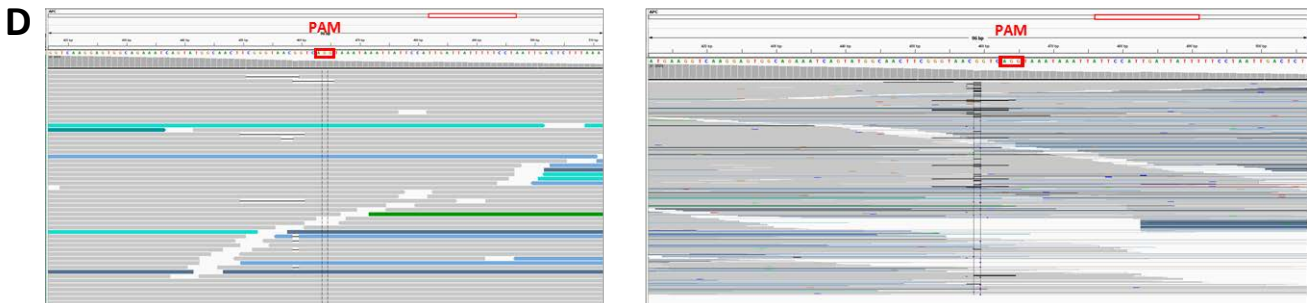
**PTEN**



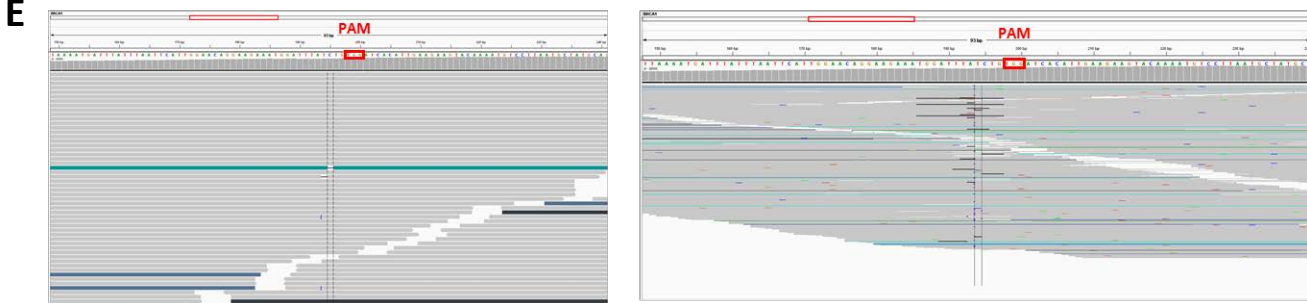
**KRAS**



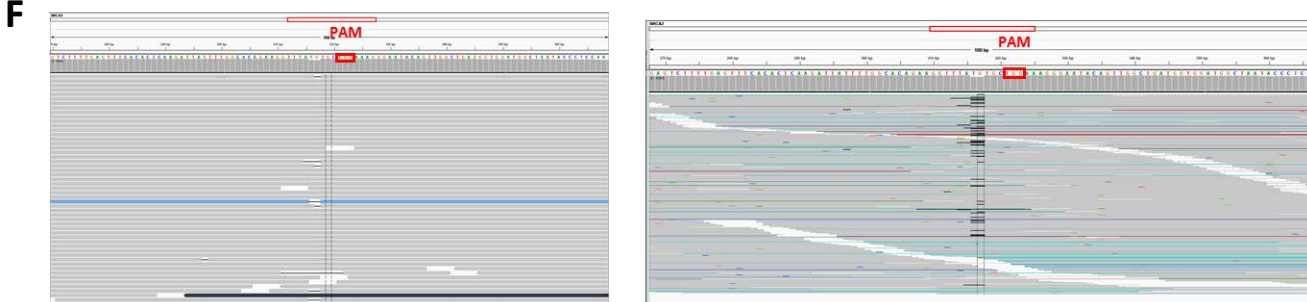
**APC**

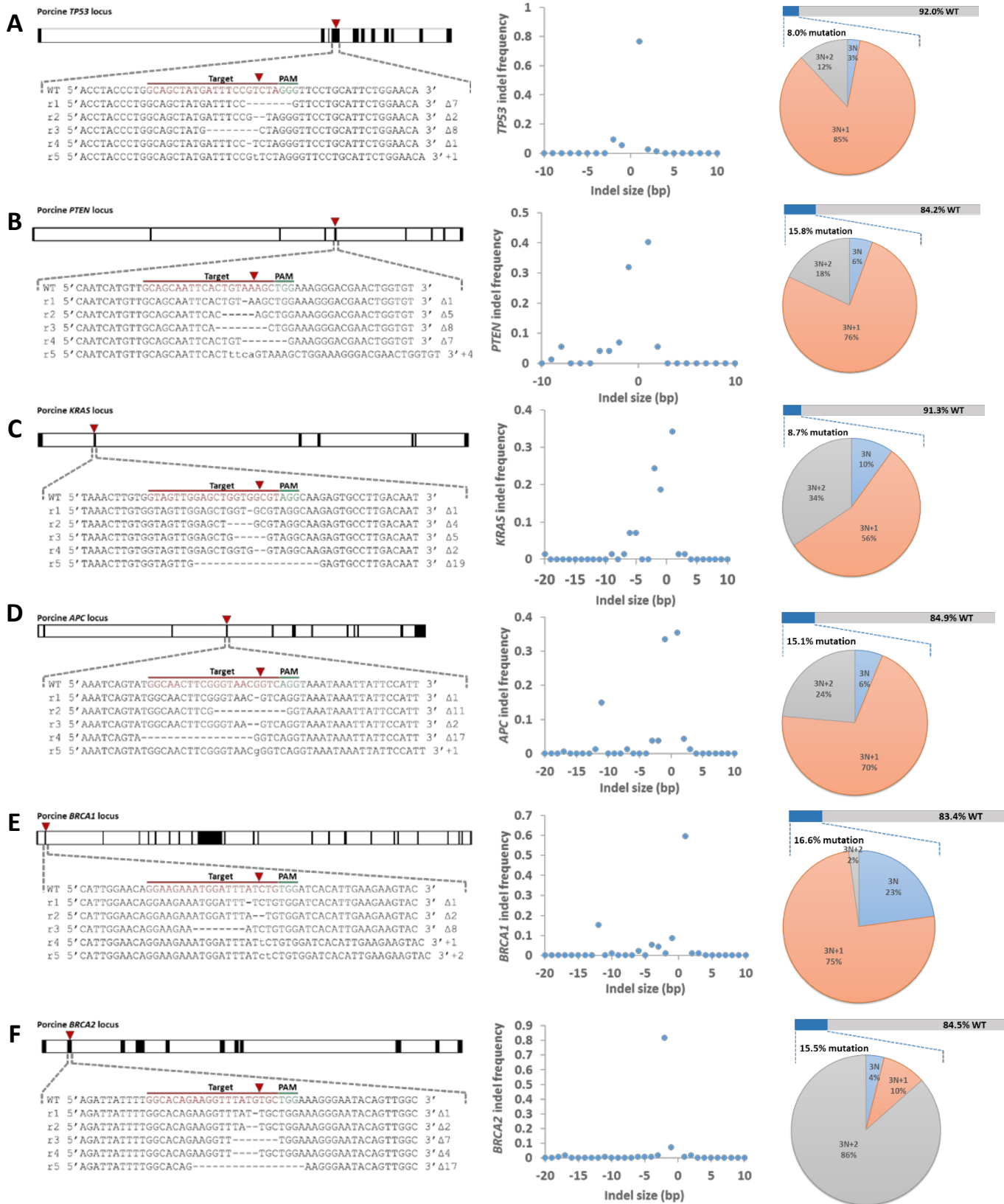


**BRCA1**



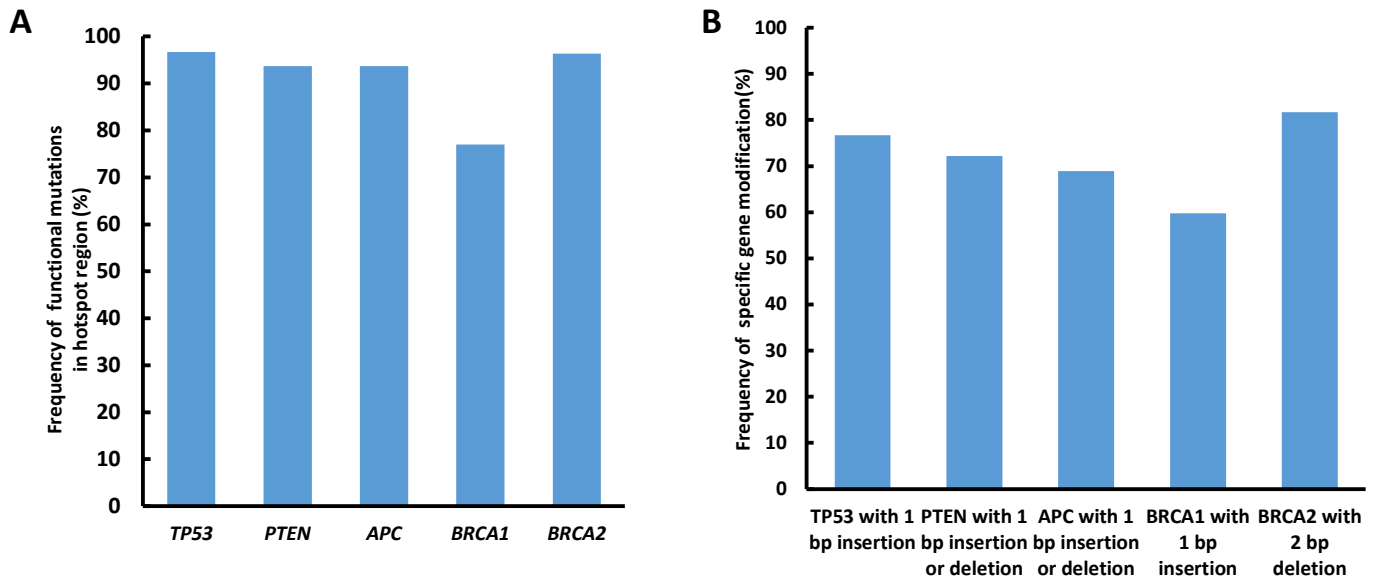
**BRCA2**



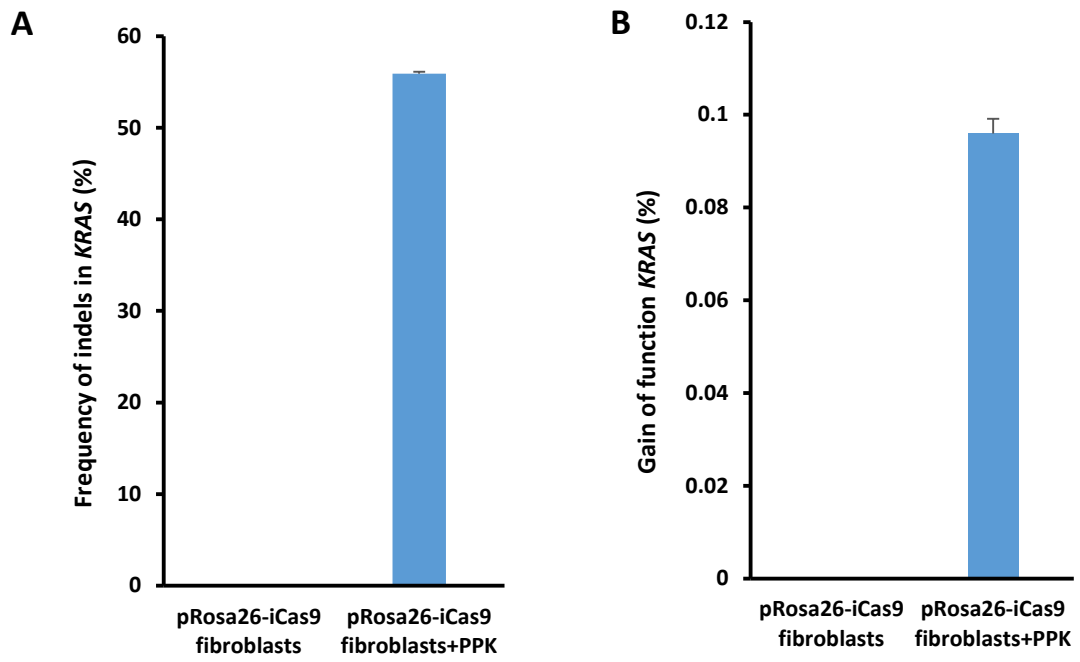


**Supplemental Figure 12.** Original deep sequencing results of *TP53* (A), *PTEN* (B), *KRAS* (C), *APC* (D), *BRCA1* (E), and *BRCA2* (F) from the sectioned primary lung tumors of Cre-dependent Cas9 expressing pigs infected with lentivirus PPK and AB12.

**Supplemental Figure 13.** Mutation analysis in autochthonous lung tumors. (A-F) (Left) sgRNAs were designed to target porcine *TP53* (A), *PTEN* (B), *KRAS* (C), *APC* (D), *BRCA1* (E), and *BRCA2* (F) loci. Moreover, five representative deep sequencing reads (r1–r5) from the lung tissues of Cre-dependent Cas9 expressing pigs infected with lentivirus PPK and AB12 showed that the formation of indels at the all six target sites. (Middle) Diagrams analyzed indel length distribution at all six sgRNAs targeting sites. (Right) Calculation of mutation efficiency and patterns ( $3N$ ,  $3N + 1$ ,  $3N + 2$ ) in sectioned lung tumors.



**Supplemental Figure 14.** Gain of function mutation analysis in autochthonous lung tumors. (A, B) The frequency functional mutations and specific indels in hotspot regions of the tumor suppress genes *TP53*, *PTEN*, *APC*, *BRCA1* and *BRCA2*).



**Supplemental Figure 15.** Initial *KRAS* mutation frequency in p*Rosa26*-iCas9 fibroblasts infected with lentivirus PPK.